2011 American Control Conference
on O'Farrell Street, San Francisco, CA, USA
June 29 - July 01, 2011

# Boundary Control of Two-Phase Fluid Flow Using the Laplace-Space Domain

Snezana Djordjevic, Okko H. Bosgra, and Paul M.J. Van den Hof

*Abstract*— **In this paper, we introduce the Laplace-space approach to a linearized two-phase flow model governed by a set of hyperbolic-like partial differential equations (PDEs). Compared to the discretization approaches to PDEs, which result in a large number of ordinary differential equations (ODEs), the Laplace-space approach gives a set of functional relationships that describe the two-phase flow behavior with respect to space. The key element in our work is the Laplace-space representation of the two-phase flow model that connects the two-phase flow regimes and causal input/output structures. The causal input/output structures need to be determined in order to design a boundary controller that can regulate the flow. The main advantage of the Laplace-space approach to the two-phase flow and effectiveness of the proposed boundary control design are illustrated on a numerical example of a counter-current two-phase flow in a vertical bubble column.**

## I. INTRODUCTION

In the chemical industry, many processes involve two-phase flow systems. Some of the most studied examples are the Fischer-Tropsch synthesis for conversion of carbon monoxide and hydrogen into petroleum substitutes, the hydrocarbonation of natural gas in pipelines, the injection of steam into oil wells for enhanced oil recovery, the boiling water in nuclear reactors, and the production of enzymes and drugs in fermentors. The main objective in most of these problems is to stabilize the flow around an operational profile, i.e., flow regime. The benefit for the chemical industry that can be gained from applying the flow control strategy to achieve this objective is enormous. However, the problem of controlling and modeling the two-phase flow systems is extremely complex and involved. For the advanced flow control designs of single-phase flow systems, we refer to [1], [2], [3]. To acquire and expand the core of the fluid flow problem to the two-phase flow, it is important to integrate the interdisciplinary areas and place an engineering perspective into control designs for the two-phase flow systems.

Concerning modeling of the two-phase flow systems, many contributions have been presented in the multiphase flow community, ranging from fundamental studies [4], [5] to studies focused on specific flow regimes [6], [7], [8], [9]. Most of these currently used two-phase flow models require specific algorithms, computational fluid dynamics (CFD), due to the complex nature of the governing equations [10], [11]. Such CFD models require advanced modeling tools, in which the relevant flow can be considered when designing the control algorithms. Nevertheless in the multiphase flow community, there is a common agreement that the pure two-phase fluid transport has to be governed by a set of first-order hyperbolic PDEs [7], [5], [12]. Basically, this means that the transport phenomena of the two-phase flow represent delays of the fluid properties from one point in space to another, whereas the interactive terms between the phases represent dissipation and/or instabilities of the flow. This is an important aspect of the two-phase flow as it gives a new perspective on a structural control of the two-phase flow systems governed by the hyperbolic PDEs. The first step in this direction is presented in [13].

In the control community, the first-order hyperbolic PDEs have been widely studied over the last two decades. The examples include control methods for the hyperbolic PDE systems such as heating in tubular reactors [14], [15] and flow in channels [16], [17]. The conventional approach to the PDE systems is to discretize the system equations and then apply the control theory for ODE systems [18], or alternatively to derive an analytical solution to a spatially distributed input using spatially distributed operators [19], [20]. Recent results extend the existing control approaches to stabilization of the hyperbolic PDE systems, proposing a frequency domain approach to control the hyperbolic PDE systems [21], [22]. This frequency approach gives a more generalized description of a boundary actuation strategy, which does not rely on the accuracy of the chosen discretization method. The work presented in [22] demonstrates the usefulness of the classical frequency domain approach and functional relationships for analysis and control of a channel flow system represented by a set of hyperbolic PDEs. The frequency approach to the hyperbolic PDEs eventually leads to an easy-to-implement algorithm for the fluid flow control.

In this paper, we introduce a theoretical framework for the boundary control of the two-phase flow based on the Laplace transformation of the governing hyperbolic-like PDEs. For the derivation of the two-phase flow model, we refer to [13] and references therein. The main contribution is in the Laplace representation of the two-phase flow model, which connects the flow regimes and causal input/output structures. From the derived causal input/output structures, the boundary control design easily follows.

The paper is organized as follows: Section II introduces a nonlinear and linearized two-phase flow model. In Section III, the Laplace transform of the linearized two-phase flow model is derived for different boundary control designs. In

Snezana Djordjevic was with the Delft Center for Systems and Control, Delft University of Technology, Mekelweg 2, 2628 CD Delft, The Netherlands and is now with the Control Systems Technology group, Eindhoven University of Technology, The Netherlands s.djordjevic@tue.nl.

Okko H. Bosgra and Paul M.J. Van den Hof are with the Delft Center for Systems and Control, Delft University of Technology, Mekelweg 2, 2628 CD Delft, The Netherlands.

978-1-4577-0081-1/11/$26.00 ©2011 AACC

Section IV, we demonstrate the effectiveness of one of the proposed boundary control designs on a counter-current two-phase flow in a vertical bubble column. Finally, Section V states the conclusions of this paper.

## II. ONE-DIMENSIONAL TWO-PHASE FLOW MODEL

### A. Nonlinear Model

We consider a one-dimensional incompressible two-phase flow in a vertical bubble column with an interfacial pressure and a drag force as the only coupling terms between two phases: gas and liquid [13]. The proposed two-phase flow model can be written in a matrix form as

$$\mathbf{E}\frac{\partial \Phi}{\partial t} + \mathbf{A}(\Phi)\frac{\partial \Phi}{\partial x} = \mathbf{c}(\Phi), \tag{1}$$

in which $\Phi = \begin{bmatrix} \alpha_g & v_g & v_l \end{bmatrix}^T$ is the vector of fluid variables, where $\alpha_g$ is the volume fraction of the gas phase, $v_g$ is the velocity of the gas phase, and $v_l$ is the velocity of the liquid phase. The matrices

$$\mathbf{E} = \begin{bmatrix} 1 & 0 & 0 \\ 0 & \rho_g & -\rho_l \\ 0 & 0 & 0 \end{bmatrix}, \tag{2}$$

and

$$\mathbf{A}(\Phi) = \begin{bmatrix} v_g & \alpha_g & 0 \\ C_p\,\rho_l\,(v_g - v_l)^2 & \rho_g v_g & -\rho_l v_l \\ v_g - v_l & \alpha_g & 1-\alpha_g \end{bmatrix}, \tag{3}$$

are the system matrices, and

$$\mathbf{c}(\Phi) = \begin{bmatrix} 0 \\ -(\rho_g - \rho_l)g - (v_g - v_l)\left(\frac{\beta}{\alpha_g} + \frac{\beta}{1-\alpha_g}\right) \\ 0 \end{bmatrix}, \tag{4}$$

is the force vector, where $\rho_g$ is the density of the gas phase, $\rho_l$ is the density of the liquid phase, $C_p$ is the interfacial pressure coefficient, and $g$ is the gravitational acceleration [13]. The term $\beta$ in $\mathbf{c}(\Phi)$ is defined by the following closure equation

$$\beta = \frac{3C_d}{4d_b}\alpha_g\alpha_l\rho_l|v_g - v_l|,$$

where $C_d$ is the drag coefficient and $d_b$ is the diameter of a single bubble (i.e., particle of a discrete phase). Most of the closure relations for the drag force are of empirical nature or include some heuristic elements which can not be deduced completely from the first principles [12].

### B. Linearized Model

This section gives a short overview of the linearized two-phase flow model which can be used to derive causal input/output structures for the two-phase flow systems described by (1). The same linearization technique has also been used to derive the linearized single-phase flow model based on the Navier-Stokes equations [2].

The linearization of (1) leads to the following linear model in terms of flow perturbations

$$\mathbf{E}\frac{\partial \Phi'}{\partial t} + \mathbf{A}(\overline{\Phi})\frac{\partial \Phi'}{\partial x} + \mathbf{A}(\Phi')\frac{\partial \overline{\Phi}}{\partial x} = \mathbf{F}\Phi', \tag{5}$$

where $\overline{\Phi}$ is the steady-state solution of (1) and $\Phi'$ is the small perturbation around it. Equation (5) represents the linearized model where the steady-state solution can vary with respect to space according to $\dfrac{\partial \overline{\Phi}}{\partial x}$. If there is no variation with respect to space, i.e., $\overline{\Phi} = \text{const}$, the linearized model reduces to

$$\mathbf{E}\frac{\partial \Phi'}{\partial t} + \mathbf{A}(\overline{\Phi})\frac{\partial \Phi'}{\partial x} = \mathbf{F}\Phi', \tag{6}$$

where

$$\mathbf{A}(\overline{\Phi}) = \begin{bmatrix} \overline{v_g} & \overline{\alpha_g} & 0 \\ C_p\,\rho_l\,(\overline{v_g} - \overline{v_l})^2 & \rho_g\overline{v_g} & -\rho_l\overline{v_l} \\ \overline{v_g} - \overline{v_l} & \overline{\alpha_g} & 1-\overline{\alpha_g} \end{bmatrix},$$

and

$$\mathbf{F} = \begin{bmatrix} 0 & 0 & 0 \\ 0 & -3/2\,\frac{C_d\,\rho_l\sqrt{(\overline{v_g}-\overline{v_l})^2}}{db} & 3/2\,\frac{C_d\,\rho_l\sqrt{(\overline{v_g}-\overline{v_l})^2}}{d_b} \\ 0 & 0 & 0 \end{bmatrix}.$$

Note that $\mathbf{E}$ is a singular matrix, which means that the proposed two-phase flow model is a partial differential algebraic equation (PDAE) model. In order to eliminate the algebraic part in (5), we introduce a coordinate transformation that reduces the problem of PDAE model to PDE model. For the full description of the coordinate transformation, we refer to our previous work [13]. After the elimination of the algebraic equation, the resulting set of PDEs with decoupled directional derivatives can be written as

$$\begin{aligned} \frac{\partial}{\partial t}\begin{bmatrix} W_1 \\ W_2 \end{bmatrix} + \begin{bmatrix} \lambda_1 & 0 \\ 0 & \lambda_2 \end{bmatrix}\frac{\partial}{\partial x}\begin{bmatrix} W_1 \\ W_2 \end{bmatrix} \\ = \begin{bmatrix} c_{11} & c_{12} \\ c_{21} & c_{22} \end{bmatrix}\begin{bmatrix} W_1 \\ W_2 \end{bmatrix}, \end{aligned} \tag{7}$$

where $W_1(t,0)$ and $W_2(t,0)$ are the bottom boundary conditions, whereas $W_1(t,L)$ and $W_2(t,L)$ are the top boundary conditions as illustrated in Fig. 1 on the vertical bubble column. Depending on the flow direction, the fluid velocity can have a positive or a negative sign, which leads to different flow regimes. This means that the boundary actuation strategies can be fully determined by the signs of the eigenvalues. Fig. 1 illustrates two extreme flow regimes: co-current regime (see Fig. 1(a)) and counter-current regime (see Fig. 1(b)). The signs of the eigenvalues $\lambda_1$ and $\lambda_2$ in (7) correspond to the direction of the flow along the characteristic curves defined by two ODEs

$$\frac{dx}{dt} = \lambda_1(\overline{\Phi}), \quad \text{and} \quad \frac{dx}{dt} = \lambda_2(\overline{\Phi}).$$

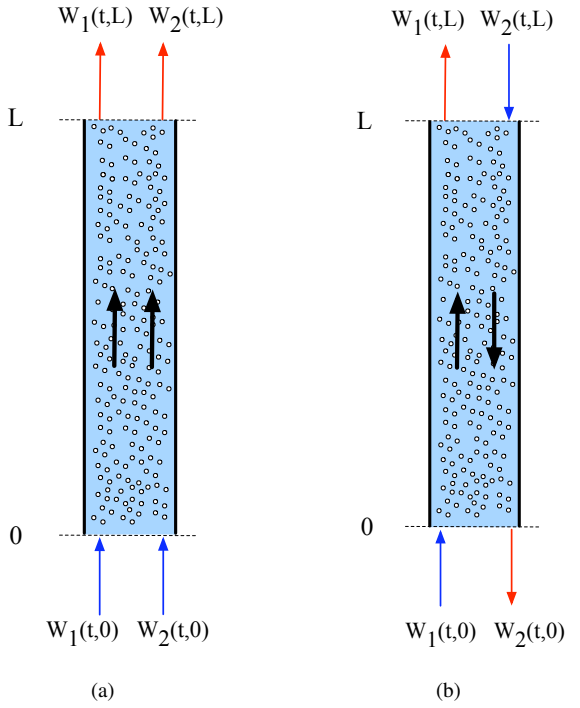


Fig. 1. Input/output structures for (a) co-current and (b) counter-current flow. The blue arrows represent the inputs while the red arrows represent the outputs.

According to the characteristic curves, the bottom boundary actuation is required for the eigenvalues $\lambda_1 > 0$ and $\lambda_2 > 0$ as illustrated in Fig. 1(a), whereas the actuation strategy with the following inputs $W_1(t,0)$ and $W_2(t,L)$ is required for the eigenvalues $\lambda_1 > 0$ and $\lambda_2 < 0$ as shown in Fig. 1(b). These boundary actuation strategies based on the eigenvalue analysis can be largely influenced by the magnitude of the coefficients on the right-hand side of (7), i.e., the drag force. This has to be taken into consideration for designing the boundary controllers for both input/output structures shown in Fig. 1.

## III. CONTROL DESIGN

### A. Boundary Control Designs

As discussed in Secion I, the main control objective for control of the two-phase flow systems is to design a controller that can be applied at one point in space to cancel the effect of fluctuations applied at the other point in space. This stabilization problem should be viewed as an structural influence of the drag force in the two-phase fluid flow system. The fluctuations in the plug flow regime according to (7) are described by the coefficients $c_{11}$, $c_{12}$, $c_{21}$, and $c_{22}$. In principle, the drag force slows down the convective flow described by the directional derivatives, i.e., the eigenvalues $\lambda_1$ and $\lambda_2$. To enforce the flow with a minimal drag force between the phases, we propose two different boundary control strategies based on the causal input/output structures illustrated in Fig. 1. The designs are based on a feedback control of the fluid flow properties at the bottom boundary $x = 0$ and top boundary $x = L$. In general, the boundary control design is possible for any system that has a hyperbolic-like behavior described by a wave that propagates from one boundary to the other [16], [17], [23].

### B. The Laplace-Space Representation of the Model

Applying the Laplace transformation to the PDE model (7) given in Section II results in the following set of equations

$$s\begin{bmatrix} W_1(s,x) \\ W_2(s,x) \end{bmatrix} + \begin{bmatrix} \lambda_1 & 0 \\ 0 & \lambda_2 \end{bmatrix} \frac{\partial}{\partial x} \begin{bmatrix} W_1(s,x) \\ W_2(s,x) \end{bmatrix} = \begin{bmatrix} c_{11} & c_{12} \\ c_{21} & c_{22} \end{bmatrix} \begin{bmatrix} W_1(s,x) \\ W_2(s,x) \end{bmatrix}. \tag{8}$$

Reordering (8) leads to a set of ODEs in the space coordinate $x$ parametrized by the Laplace variable $s$

$$\frac{d}{dx}\begin{bmatrix} W_1(s,x) \\ W_2(s,x) \end{bmatrix} = \begin{bmatrix} \lambda_1 & 0 \\ 0 & \lambda_2 \end{bmatrix}^{-1} \left( \begin{bmatrix} c_{11} & c_{12} \\ c_{21} & c_{22} \end{bmatrix} - sI \right) \begin{bmatrix} W_1(s,x) \\ W_2(s,x) \end{bmatrix}. \tag{9}$$

The advantage of the Laplace-space representation of the two-phase flow model is that (9) can be solved analytically by integrating the set of ODEs over the space domain. This gives the following relationships between the variables at the bottom boundary $x = 0$ and at any location $x$

$$\begin{bmatrix} W_1(s,x) \\ W_2(s,x) \end{bmatrix} = \exp(\mathscr{A}(s)x) \begin{bmatrix} W_1(s,0) \\ W_2(s,0) \end{bmatrix}, \tag{10}$$

where

$$\mathscr{A}(s) = \begin{bmatrix} \frac{c_{11}-s}{\lambda_1} & \frac{c_{21}}{\lambda_1} \\ \frac{c_{21}}{\lambda_2} & \frac{c_{22}-s}{\lambda_2} \end{bmatrix}.$$

### C. Coordinate Transformations

Using the following coordinate transformation

$$\begin{bmatrix} W_1(s,x) \\ W_2(s,x) \end{bmatrix} = \mathbf{Q}(s)^{-1} \begin{bmatrix} Z_1(s,x) \\ Z_2(s,x) \end{bmatrix}, \tag{11}$$

the model (9) can be written such that the dynamics of the system matrix $\mathscr{A}(s)$ are decoupled

$$\begin{bmatrix} Z_1(s,x) \\ Z_2(s,x) \end{bmatrix} = \begin{bmatrix} e^{\lambda_1^*(s)x} & 0 \\ 0 & e^{\lambda_2^*(s)x} \end{bmatrix} \begin{bmatrix} Z(s,0) \\ Z(s,0) \end{bmatrix}. \tag{12}$$

where

$$\lambda_1^*(s) = \frac{1}{2}\frac{-(\lambda_1+\lambda_2)s + \lambda_1 c_{22} + \lambda_2 c_{11} + \sqrt{\varepsilon(s)}}{\lambda_1\lambda_2},$$

$$\lambda_2^*(s) = \frac{1}{2}\frac{-(\lambda_1+\lambda_2)s + \lambda_1 c_{22} + \lambda_2 c_{11} - \sqrt{\varepsilon(s)}}{\lambda_1\lambda_2},$$

with $\varepsilon(s)$ being

$$\varepsilon(s) = ((\lambda_1-\lambda_2)s + (c_{11}\lambda_2 - \lambda_1 c_{22}))^2 + 4\lambda_1\lambda_2 c_{21}.$$

Note that $\lambda_1^*(s)$ and $\lambda_2^*(s)$ comprise the directional derivatives $\lambda_1$ and $\lambda_2$ and the coefficients $c_{11}$, $c_{12}$, $c_{21}$, and $c_{22}$.

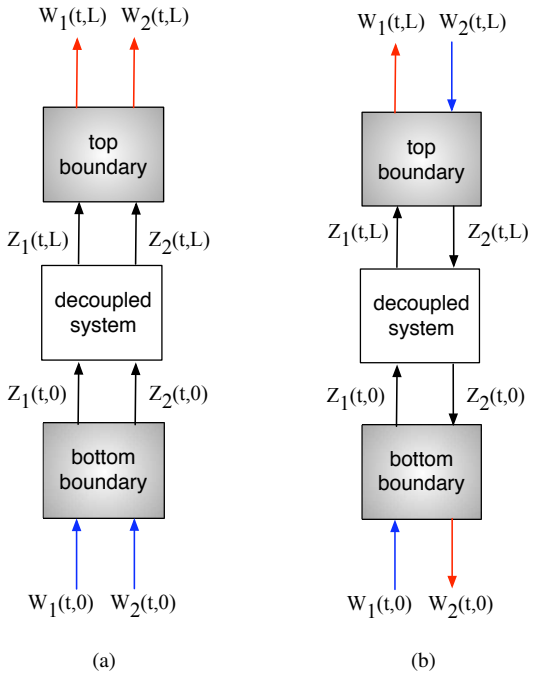


Fig. 2. Causal input/output structures for (a) co-current flow and (b) counter-current flow based on the decoupled directional derivatives. The blue arrows represent the inputs while the red arrows represent the outputs.

The transformation matrix $\mathbf{Q}(s)$ represents a matrix which contains the eigenvectors corresponding to the eigenvalues $\lambda_1^*(s)$ and $\lambda_2^*(s)$ in the right order

$$\mathbf{Q}(s) = \begin{bmatrix} q_{11}(s) & q_{12}(s) \\ q_{21}(s) & q_{22}(s) \end{bmatrix},$$

where

$$q_{11}(s) = 1, \qquad q_{21}(s) = 1,$$
$$q_{12}(s) = \frac{1}{2}\frac{1}{c_{21}\lambda_1}\left(\lambda_2 c_{11} - \lambda_1 c_{22} + (\lambda_1 - \lambda_2)s + \sqrt{\varepsilon(s)}\right),$$
$$q_{22}(s) = -\frac{1}{2}\frac{1}{c_{21}\lambda_1}\left(-\lambda_2 c_{11} + \lambda_1 c_{22} - (\lambda_1 - \lambda_2)s + \sqrt{\varepsilon(s)}\right).$$

It is important to observe that the signs of $\lambda_1^*(s)$ and $\lambda_2^*(s)$ precisely determine the causal input/output structures for the linearized two-phase flow as illustrated in Fig. 2. The causal input/output structures can be viewed as extensions of the system boundaries to their surroundings as shown in Fig. 2. The top and bottom boundary blocks represent the coordinate transformations between the coordinates which can be recovered following the causal flow directions. The original coordinate system $\begin{bmatrix} W_1(s,x) & W_2(s,x) \end{bmatrix}^{\mathrm{T}}$ can be recovered following the flow in the boundary blocks as illustrated in Fig. 2 for both flow regimes.

*1) Co-current flow:* Suppose that $\lambda_1^*(s) < 0$ and $\lambda_2^*(s) < 0$, then the inputs have to be defined at $x = 0$ and the outputs at $x = L$ (see Fig. 2(a)). In this case, according to (13), the connections between the inputs $Z_1(s,0)$ and $Z_2(s,0)$, and the outputs $Z_1(s,L)$ and $Z_2(s,L)$ are defined by the delay functions $\mathrm{e}^{\lambda_1^*(s)L}$ and $\mathrm{e}^{\lambda_2^*(s)L}$, respectively. Then, the two-phase flow model for the co-current flow in the $\begin{bmatrix} Z_1(s,x) & Z_2(s,x) \end{bmatrix}^{\mathrm{T}}$ coordinate system has the causal input/output structure which can be written as

$$\begin{bmatrix} Z_1(s,L) \\ Z_2(s,L) \end{bmatrix} = \begin{bmatrix} \mathrm{e}^{\lambda_1^*(s)L} & 0 \\ 0 & \mathrm{e}^{\lambda_2^*(s)L} \end{bmatrix} \begin{bmatrix} Z(s,0) \\ Z(s,0) \end{bmatrix}. \tag{13}$$

The coordinate system $\begin{bmatrix} W_1(s,x) & W_2(s,x) \end{bmatrix}^{\mathrm{T}}$ can be recovered according to the input/output structure shown in Fig. 2(a) as

$$\begin{bmatrix} W_1(s,L) \\ W_2(s,L) \end{bmatrix} = \mathbf{G}_{\mathrm{co}}(s) \begin{bmatrix} W_1(s,0) \\ W_2(s,0) \end{bmatrix}, \tag{14}$$

where

$$\mathbf{G}_{\mathrm{co}}(s) = \mathbf{Q}^{-1}(s) \begin{bmatrix} \mathrm{e}^{\lambda_1^*(s)x} & 0 \\ 0 & \mathrm{e}^{\lambda_2^*(s)x} \end{bmatrix} \mathbf{Q}(s).$$

*2) Counter-current flow:* Suppose that the same input/output structure holds for the eigenvalues $\lambda_1^*(s) > 0$ and $\lambda_2^*(s) < 0$, then the first equation in (13) is the inverse of the time delay function which is not physically realizable. In terms of dynamics, it defines a non-causal relation between the properties at the top and bottom boundaries. This means that the wave with $\lambda_1^*(s) > 0$ propagates in the opposite spatial direction from the predicted one, i.e., from top to bottom. By the following reordering, we can obtain a stable wave propagation and a causal input/output structure

$$\begin{bmatrix} Z_1(s,0) \\ Z_2(s,L) \end{bmatrix} = \begin{bmatrix} \mathrm{e}^{-\lambda_1^*(s)L} & 0 \\ 0 & \mathrm{e}^{\lambda_2^*(s)L} \end{bmatrix} \begin{bmatrix} Z(s,L) \\ Z(s,0) \end{bmatrix}. \tag{15}$$

Fig. 2(b) illustrates the inversion that is also known as bilateral coupling [24]. Essentially, the inversion of the relationship between the input and output brings the set of equations (13) to the causal input/output structure. Now, the bottom boundary can be recovered as

$$\begin{bmatrix} Z_1(s,0) \\ W_2(s,0) \end{bmatrix} = \begin{bmatrix} q_{11}(s) - \frac{q_{12}(s)q_{21}(s)}{q_{22}(s)} & \frac{q_{12}(s)}{q_{22}(s)} \\ -\frac{q_{21}(s)}{q_{22}(s)} & \frac{1}{q_{22}(s)} \end{bmatrix} \begin{bmatrix} W_1(s,0) \\ Z_2(s,0) \end{bmatrix}, \tag{16}$$

whereas the top boundary can be recovered as

$$\begin{bmatrix} W_1(s,L) \\ Z_2(s,L) \end{bmatrix} = \begin{bmatrix} \frac{1}{q_{11}(s)} & -\frac{q_{12}(s)}{q_{11}(s)} \\ \frac{q_{21}(s)}{q_{11}(s)} & q_{22}(s) - \frac{q_{12}(s)q_{21}(s)}{q_{11}(s)} \end{bmatrix} \begin{bmatrix} Z_1(s,L) \\ W_2(s,L) \end{bmatrix}. \tag{17}$$

Using the linear combination of the given boundaries (16) and (17), the original coordinates can be fully recovered as

$$\begin{bmatrix} W_1(s,0) \\ W_2(s,L) \end{bmatrix} = \mathbf{G}_{\mathrm{cc}}(s) \begin{bmatrix} W_1(s,L) \\ W_2(s,0) \end{bmatrix}, \tag{18}$$

where

$$\mathbf{G}_{\mathrm{cc}}(s) = \begin{bmatrix} q_{11}(s) & -q_{12}(s)\mathrm{e}^{-\lambda_1^*(s)} \\ q_{21}(s)\mathrm{e}^{\lambda_2^*(s)} & -q_{22}(s) \end{bmatrix}^{-1} \begin{bmatrix} q_{11}\mathrm{e}^{-\lambda_1^*(s)} & -q_{12}(s) \\ q_{21}(s) & -q_{22}(s)\mathrm{e}^{\lambda_2^*(s)} \end{bmatrix}.$$

Equation (18) represents the causal input/output structure between the properties at the boundaries written in $\left[\begin{array}{cc} W_1(s,x) & W_2(s,x) \end{array}\right]^{\mathrm{T}}$ coordinates, where the system dynamics are described by the elements of $\mathbf{G}_{\mathrm{cc}}(s)$.

According to the elements of the transformation matrix $\mathbf{Q}(s)$, which are irrational functions, the elements of $\mathbf{G}_{\mathrm{co}}(s)$ and $\mathbf{G}_{\mathrm{cc}}(s)$ are also irrational functions which need to be approximated using the Padé approximations. The Padé approximations can take on many increasingly complicated forms, depending upon the degree of accuracy required. In Section IV, we will present some numerical results and the Padé approximations for the counter-current flow described by $\mathbf{G}_{\mathrm{cc}}(s)$.

### D. Boundary Controller

Due to the simple algebraic expressions of $\mathbf{G}_{\mathrm{co}}(s)$ and $\mathbf{G}_{\mathrm{cc}}(s)$, the behavior of the two-phase flow in the Laplace-space domain can be easily observed with a little computational effort. The computational complexity associated with the complex CFD models can be greatly simplified by making use of the theory associated with the rational transfer functions and the Padé approximations. The simulation time required for rational transfer functions in Matlab is just a few seconds. This is a huge advantage of the Laplace-space representation of the two-phase flow model.

The boundary control law can be derived for the Laplace-space model representation of the two-phase flow using the following conditions for

*1) Co-current flow:*

$$\left[\begin{array}{c} W_1(s,L) \\ W_2(s,L) \end{array}\right] = \left[\begin{array}{cc} K_{11} & K_{12} \\ K_{21} & K_{22} \end{array}\right] \left[\begin{array}{c} W_1(s,0) \\ W_2(s,0) \end{array}\right] \tag{19}$$

*2) Counter-current flow:*

$$\left[\begin{array}{c} W_1(s,0) \\ W_2(s,L) \end{array}\right] = \left[\begin{array}{cc} K_{11} & K_{12} \\ K_{21} & K_{22} \end{array}\right] \left[\begin{array}{c} W_1(s,L) \\ W_2(s,0) \end{array}\right]. \tag{20}$$

The boundary conditions (19) and (20) contain the tunable control parameters $K_{11}$, $K_{12}$, $K_{21}$, and $K_{22}$ that can drive the two-phase flow in a desirable manner ensuring the stabilization of the specific flow regimes illustrated in Fig. 1.

## IV. NUMERICAL SIMULATIONS

In this section, we give simulation results of an uncontrolled and controlled two-phase flow based on the derived model given as (7) for the counter-current flow illustrated in Fig. 1(b). The system parameters are given in Table I.

Fig. 3 compares the uncontrolled and controlled flow with the exact solution and approximated solution. The exact solution is replaced by the Padé approximation. The causal interconnections can be viewed as extensions of the system boundaries to their surroundings as shown in Fig. 2. The top and bottom boundary blocks represent the coordinate transformations between the coordinates which can be recovered following the causal flow directions. In the example shown in Fig. 3, we use the fourth-order Padé approximation.

TABLE I

FLUID PROPERTIES AND SYSTEM PARAMETERS.

| Symbol | Value |
|---|---|
| $\lambda_1$ | 0.0954 |
| $\lambda_2$ | -0.064 |
| $c_{11}$ | 521 |
| $c_{12}$ | 1647 |
| $c_{21}$ | -521 |
| $c_{22}$ | -1647 |

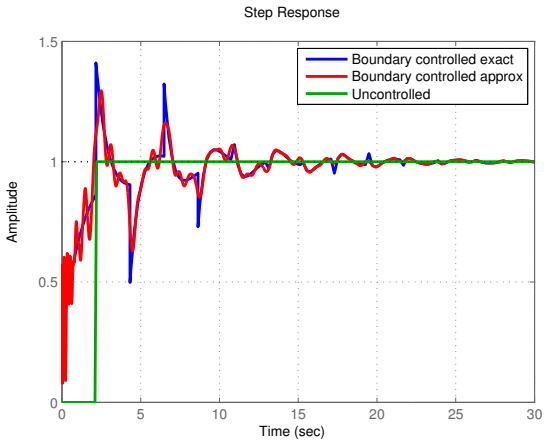


Fig. 3. Step responses for an uncontrolled and controlled flow with the proportional gain $K_{11} = 0.3$ for the exact and approximated solutions of the controlled flow using the fourth-order Padé approximation.

As can be seen, the boundary controller for the upward propagation can push the flow faster from one side of the boundary to the other side with fluctuations that fade out with respect to time. The fluctuations are mainly caused by the drag force which can be suppressed by tuning $K_{11}$ for the internal delay function as illustrated in Fig. 2. The plug flow that is created in this way has to travel with the shortest possible time from one boundary to the other boundary. This means that the controller has to place the eigenvalue $\lambda_1^*(s)$ closer to zero, since this would mean that there is almost no delay of the fluid properties between the boundaries. Fig. 4 shows the control results obtained applying the proportional gain $K_{11}$ at the boundaries that can achieve this goal. Due to the fact that the value $e^{\lambda_2^*(s)L}$ is rather small, the effect of the flow in the opposite direction can be neglected.

To demonstrate the effectiveness of the boundary controller, we also compare the controlled model with the drag force and without the drag force. Fig. 5 illustrates the simulation results. The controller is applied on two cases: with the drag force described by the coefficients $c_{11}$, $c_{12}$, $c_{21}$, and $c_{22}$ and without the drag force where the coefficients $c_{11} = c_{12} = c_{21} = c_{22} = 0$. As can be seen, the proposed boundary controller minimizes the effect of the drag force almost completely.

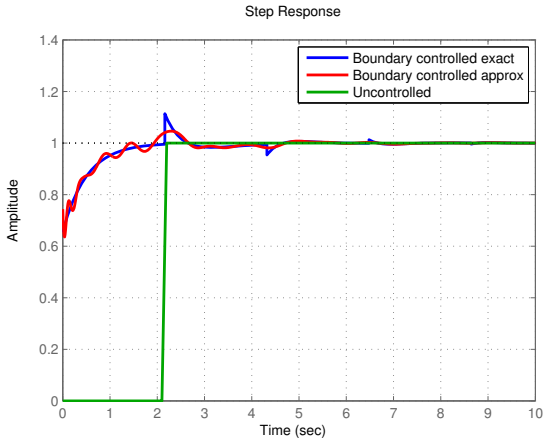


Fig. 4. Step responses for an uncontrolled and controlled flow with the proportional gain $K_{11} = 1.8$ for the exact and approximated solutions of the controlled flow using the fourth-order Padé approximation.

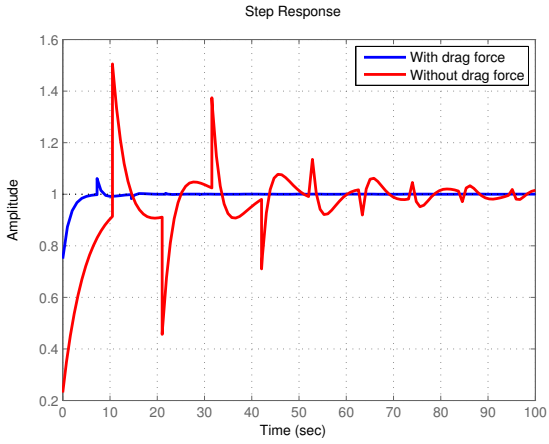


Fig. 5. The time responses of the controlled flow with and without the drag force for the wave that propagates from the bottom.

## V. CONCLUSIONS

In this paper, we have presented a theoretical framework for the boundary control of the two-phase flow system discussed in [13]. The given framework establishes the analysis of causal input/output structures for the two-phase flow systems, and proposes a new modeling approach based on the Laplace-space representation of the two-phase flow model. The main advantage of the Laplace approach is that it guarantees the causality of the input/output structures for a wide range of operating regimes, and it provides insights needed for the derived boundary control design. The main contribution of the paper includes an implementable boundary control design for a uniform flow regime of the two-phase flow in the vertical bubble column that can be extended for more complex flow cases.

## VI. ACKNOWLEDGMENTS

The authors would like to thank the anonymous reviewers of this paper for their constructive comments and valuable suggestions.

## REFERENCES

[1] T. Bewley, "Flow control: new challenges for a new renaissance," *Progress in Aerospace Sciences*, vol. 37, no. 1, pp. 21–58, 2001.
[2] O. Aamo and M. Krstić, *Flow control by feedback: stabilization and mixing*. Springer Verlag, 2003.
[3] M. Jovanovic and B. Bamieh, "Componentwise energy amplification in channel flows," *Journal of Fluid Mechanics*, vol. 534, pp. 145–183, 2005.
[4] D. Dankworth and S. Sundaresan, "Time-dependent vertical gas-liquid flow in packed beds," *Chemical Engineering Science*, vol. 47, pp. 337–46, 1992.
[5] M. Ishii and T. Hibiki, *Thermo-fluid dynamics of two-phase flow*. Springer, 2006.
[6] A. Biesheuvel and L. Wijngaarden, "Two-phase flow equations for a dilute dispersion of gas bubbles in liquid," *Journal of Fluid Mechanics*, vol. 148, pp. 301–18, 1984.
[7] V. Ransom and D. Hicks, "Hyperbolic two-pressure models for two-phase flow," *J. Comput. Phys*, vol. 53, no. 1, pp. 124–151, 1984.
[8] S. Gharat and J. Joshi, "Transport phenomena in bubble column reactors I: Flow pattern," *The chemical engineering journal*, vol. 48, no. 3, pp. 141–151, 1992.
[9] W.-D. Deckwer, *Bubble Column Reactors*. Wiley, 1992.
[10] H. Jakobsen, B. Sannæs, S. Grevskott, and H. Svendsen, "Modeling of bubble driven vertical flows," *Ind. Eng. Chem. Res*, vol. 36, pp. 4052–4074, 1997.
[11] D. Lathouwers, "Modelling and simulation of turbulent bubbly flow," Ph.D. dissertation, Delft University of Technology, The Netherlands, 1999.
[12] J. Park, D. Drew, and R. Lahey, Jr, "The analysis of void wave propagation in adiabatic monodispersed bubbly two-phase flows using an ensemble-averaged two-fluid model," *International Journal of Multiphase Flow*, vol. 24, no. 7, pp. 1205–1244, 1999.
[13] S. Djordjevic, O. Bosgra, P. Van den Hof, and D. Jeltsema, "Boundary Actuation Structure of Linearized Two-Phase Flow," in *American Control Conference, 2010. Proceedings of the 2010*, 2010, pp. 3759–3764.
[14] H. Sano, "Exponential stability of a mono-tubular heat exchanger equation with output feedback," *Systems & control letters*, vol. 50, no. 5, pp. 363–369, 2003.
[15] P. Christofides and P. Daoutidis, "Feedback control of hyperbolic PDE systems," *AIChE Journal*, vol. 42, no. 11, pp. 3063–3086, 1996.
[16] J. De Halleux, C. Prieur, J. Coron, B. d'Andrea Novel, and G. Bastin, "Boundary feedback control in networks of open channels," *Automatica*, vol. 39, no. 8, pp. 1365–1376, 2003.
[17] G. Bastin, J. Coron, and B. d'Andrea Novel, "Boundary feedback control and Lyapunov stability analysis for physical networks of $2\times 2$ hyperbolic balance laws," in *47th IEEE Conference on Decision and Control, 2008. CDC 2008*, 2008, pp. 1454–1458.
[18] R. D'Andrea and G. Dullerud, "Distributed control design for spatially interconnected systems," *IEEE Transactions on Automatic Control*, vol. 48, no. 9, pp. 1478–1495, 2003.
[19] M. Krstic and A. Smyshlyaev, "Backstepping boundary control for first-order hyperbolic PDEs and application to systems with actuator and sensor delays," *Systems & Control Letters*, vol. 57, no. 9, pp. 750–758, 2008.
[20] P. Christofides, *Nonlinear and robust control of PDE systems: methods and applications to transport-reaction processes*. Birkhauser, 2001.
[21] S. Munier, X. Litrico, G. Belaud, and P. Malaterre, "Distributed approximation of open-channel flow routing accounting for backwater effects," *Advances in Water Resources*, vol. 31, no. 12, pp. 1590–1602, 2008.
[22] X. Litrico and V. Fromion, "Boundary control of hyperbolic conservation laws using a frequency domain approach," *Automatica*, vol. 45, no. 3, pp. 647–656, 2009.
[23] M. Krstic and A. Smyshlyaev, "Boundary control of PDEs," 2008.
[24] H. Paynter, *Analysis and design of engineering systems*. MIT press Cambridge, Mass., 1961.